Low-temperature ordered states of $R\mathrm{Rh}_4\mathrm{B}_4$ (R = rare earth) due to dipole-dipole and exchange interactions

Sushil K. Misra

Physics Department, Concordia University, 1455 de Maisonneuve Boulevard West, Montreal, Quebec, Canada H3G 1M8

H. Postma

Laboratorium voor Technische Natuurkunde, Technische Hogeschool Delft, Postbus 5046, 2600-GA Delft, The Netherlands

(Received 27 December 1983)

Low-temperature ordered states of ternary rare-earth rhodium borides $R\mathrm{Rh}_4\mathrm{B}_4$ (where R denotes rare earth) have been investigated by the use of the Luttinger-Tisza method, taking into account both the dipole-dipole and exchange interactions. It is found that, with suitable values of exchange constants, it is possible to explain the observed orderings of all the compounds. An estimate has also been made of the internal magnetic fields produced due to magnetic ordering of rare-earth metal ions at a rhodium site. These values are small, and might permit coexistence of magnetic ordering and superconductivity.

I. INTRODUCTION

Considerable theoretical and experimental interest has recently been expressed in the ternary rare-earth rhodium boride compounds $R\mathrm{Rh}_4\mathrm{B}_4$ (hereafter TRRB, where R denotes rare earth; see, e.g., Ref. 1, for a detailed coverage; $_{57}$La, $_{58}$Ce, $_{59}$Pr, and $_{70}$Yb do not form TRRB structures).

Many TRRB compounds exhibit the coexistence of superconductivity and long-range antiferromagnetic order.[2-11] These are $R\mathrm{Rh}_4\mathrm{B}_4$, where R denotes $_{62}$Sm, $_{60}$Nd, and $_{69}$Tm. On the other hand, when ferromagnetic ordering prevails at low temperatures, the superconducting state is destroyed for R denoting $_{64}$Gd, $_{65}$Tb, $_{66}$Dy, $_{67}$Ho, and $_{68}$Er.[12,13]

Another interesting aspect of the problem is the estimation of the magnetic fields at a rhodium site as produced by the magnetic ordering of the rare-earth (RE) ions. Since the $3d$ electrons of Rh atoms are responsible for superconductivity, it is conceivable that if the magnetic field at Rh sites is not sufficiently large, the superconductivity may not be quenched by the magnetic field due to the ordered RE sublattice, thus allowing the coexistence of superconductivity and magnetic ordering. (Of course, the exchange interaction of the rare-earth ions with the conduction electrons is also sufficiently small at the same time; otherwise the exchange interaction alone can destroy the superconductivity.)

Recently, numerous efforts have been made to understand various aspects of superconductivity and magnetic ordering of TRRB compounds.[14-21] In addition, many works have appeared dealing with the details of the crystal fields in TRRB compounds.[22-27]

It is our purpose in this paper to study the low-temperature magnetic ordering of TRRB compounds as it is affected by the dipole-dipole and exchange interactions between the RE ions. The method used is that originally proposed by Luttinger and Tisza[28] (hereafter LT), and further extended using permutation groups.[29] The required g values, which are not known experimentally, are

those computed on the basis of the Hund's-rule ground state of RE ions located on a body-centered-tetragonal sublattice. As well, the values of the various RE-RE exchange interactions are not known; however, a limit can be set if the predicted ordered states are to be in agreement with those observed experimentally. Other interactions, e.g., Ruderman-Kittel-Kasuya-Yosida (RKKY) interactions, described in Sec. II, will not be taken into account here. These are presumably responsible for the finer spatial variation of the orderings. It is hoped that this study will supplement the ongoing efforts toward complete understanding of the coexistence of superconductivity and magnetic ordering of TRRB compounds at lower temperatures.

Section II contains a brief review of the experimental results as far as the magnetic orderings are concerned. The crystal structure of TRRB compounds is described in Sec. III. The details of the LT method as it applies to our investigation are given in Sec. IV. Section V contains the calculation of the g factors for the various RE ions in TRRB lattices. The predicted orderings and their comparison with the experimental ones are presented in Sec. VI. The estimation of the magnetic field at a Rh site is the subject of Sec. VII. Concluding remarks are made in Sec. VIII.

II. EXPERIMENTAL RESULTS

Experimentally, TRRB compounds are found to undergo either ferromagnetic or antiferromagnetic orderings at low temperatures, with or without coexistence of superconductivity. As far as the compounds $R = _{59}$Pr, $_{61}$Pm, and $_{63}$Eu are concerned, no magnetic ordering has yet been observed experimentally. Ferromagnetic ordering without coexistence of superconductivity has been observed in the compounds $R = _{65}$Tb, $_{66}$Dy, $_{67}$Ho, and $_{68}$Er,[16,18] with their easy axes of magnetization along the c, c, c, and a (basal-plane) axes, respectively.[11,12,30] $R = _{64}$Gd has also been found to order ferromagnetically

at lower temperature. Antiferromagnetic ordering with coexistence of superconductivity has been observed in the compounds $R = _{60}Nd$, $_{62}Sm$, and $_{69}Tm$.[9,16,20,31] In addition, $_{71}LuRh_4B_4$ also shows superconductivity.

The sublattice of RE ions (body-centered tetragonal) undergoes long-range magnetic ordering as evidenced by sharp magnetic ordering temperatures T_M and well-defined features in the physical properties at T_M. With increasing RE atomic number, the low-temperature behavior switches from superconductivity for $_{60}Nd$ and $_{62}Sm$ to ferromagnetism for $_{64}Gd$, $_{65}Tb$, $_{66}Dy$, and $_{67}Ho$, and back to superconductivity for $_{68}Er$, $_{69}Tm$, and $_{71}Lu$. Moreover, all of the superconducting TRRB compounds in which the RE $4f$ electron shell is partially filled undergo some type of magnetic ordering below their superconducting transition temperatures at temperatures T_M in the vicinity of 1 K. Whereas, $R = _{68}Er$ becomes ferromagnetic, $_{60}Nd$ (Refs. 8 and 15), $_{62}Sm$ (Ref. 9), and $_{69}Tm$ (Refs. 14 and 17) exhibit antiferromagnetic transitions.

For $TmRh_4B_4$, the superconducting and long-range magnetic order coexist for temperatures less than 0.4 K,[13,14,17] while bulk superconductivity, which occurs at 9.8 K, persists to temperatures below 60 mK. The neutron-diffraction data[17] are consistent with the development of a sinusoidally modulated (along the [101] direction) antiferromagnetic structure in which the magnetic moments are aligned along the [010] direction in the superconducting state in zero applied field. As for $NdRh_4B_4$, the neutron-diffraction data[15] confirm the occurrence of two distinct phases with long-range magnetic order below the superconducting phase-transition temperature $T_{sc} = 5.4$ K. In the higher-temperature magnetic phase, for which $T_{MH} \simeq 1.5$ K, the body-centered-tetragonal sublattice of Nd moments orders antiferromagnetically with a sinusoidal modulation of the moment along the [100] direction. In the lower-temperature phase, $T_{ML} \simeq 1.0$ K, there is a change in the direction of the modulation wave vector to [110]. In both phases, the moments are aligned along the unique c axis.

$ErRh_4B_4$ exhibits reentrant superconductive behavior due to the onset of long-range ferromagnetic ordering of Er magnetic moments.[32] It becomes superconducting at an upper critical temperature T_{c1} and loses its superconductivity at a lower critical temperature T_{c2}, which is close to the Curie temperature. A first-order transition from the superconducting to the ferromagnetic normal state occurs at the lower critical temperature, as revealed by thermal hysteresis in various physical properties and a feature in the specific heat near the lower critical temperature.[33] It is ultimately the ferromagnetism that survives the struggle with superconductivity. Further neutron-scattering experiments reveal that $ErRh_4B_4$ undergoes a ferromagnetic transition below T_{c2}, and also above T_{c2} to ~ 1.2 K.[33] The experiments on $ErRh_4B_4$ have yielded evidence for a spatially inhomogeneous state in a narrow temperature interval above the lower critical temperature in which superconducting regions coexist with normal ferromagnetic regions. Moreover, within superconducting regions the Er magnetic moments are in a sinusoidally modulated magnetic state with a wavelength of the order of a few hundred angstroms. Thus the ferromagnetic

state within the superconducting regions is transformed into an oscillatory magnetic state characterized by a zero net magnetization.

The trend of the magnetic ordering temperatures, i.e., a peak at $R = _{66}Dy$ rather than at $R = _{64}Gd$, confirms that the indirect RKKY exchange interaction is a definite factor in the fine details of low-temperature ordering. The oscillatory magnetic state was first explained to be due to the RKKY indirect-exchange mechanism by Anderson and Suhl,[17,34] wherein the oscillatory character of the magnetization results from the change in q-dependent magnetic susceptibility caused by the superconductivity. Recently, Blount and Varma[35] suggested that the electromagnetic interaction between the magnetization of the localized ions and the momenta of the conduction electrons could lead to a spiral magnetization state in a ferromagnetic superconductor. Neutron-diffraction measurements on a single-crystal sample of $ErRh_4B_4$ by Sinha et al.[36] indicate that the sinusoidally modulated state is linearly polarized. On the other hand, Greenside et al.[37] have shown that, for sufficiently strong magnetic anisotropy, such a linearly polarized sinusoidal state can prevail over both spiral and vortex states. Other alternatives are laminar structure,[38] stabilized by the rare-earth magnetization in a self-consistent manner, and combined spiral magnetic and spontaneous vortex states.[39]

The superconducting electrons in TRRB compounds are d electrons (localized on Rh atoms),[21] and the exchange interaction between these electrons and RE ions is weak, which is the reason for existence of superconductivity despite a high concentration of RE ions.

III. CRYSTAL STRUCTURE OF RRh_4B_4

X-ray-diffraction data reveal that TRRB compounds are isomorphous to RCo_4B_4 system;[40,41] and can be indexed as tetragonal lattices. TRRB compounds with $R = _{57}La$, $_{58}Ce$, $_{59}Pr$, and $_{70}Yb$ do not form this phase. The transition temperatures of those TRRB compounds which exhibit superconductivity are the highest ever observed among metal-rich borides; at the same time, the $[M]/[B]$ (where M denotes metal) ratio is closer to 1.0 than any of the other superconducting borides.[42] The

TABLE I. Cell parameters of the tetragonal compound RRh_4B_4 (including Y and Lu).

Re	a (Å)[a]	c (Å)[b]	c/a
($_{39}Y$)	5.308	7.403	1.395
$_{60}Nd$	5.333	7.468	1.400
$_{62}Sm$	5.312	7.430	1.399
$_{64}Gd$	5.309	7.417	1.397
$_{65}Tb$	5.303	7.404	1.396
$_{66}Dy$	5.302	7.395	1.395
$_{67}Ho$	5.293	7.397	1.394
$_{68}Er$	5.292	7.374	1.393
$_{69}Tm$	5.287	7.359	1.392
($_{71}Lu$)	5.294	7.359	1.390

[a] ± 0.002 Å.
[b] ± 0.003 Å.
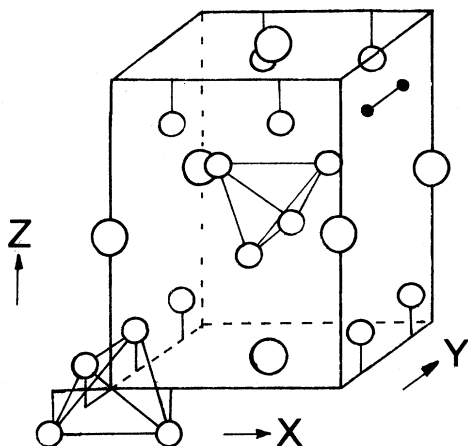
FIG. 1. Proposed structure of YRh$_4$B$_4$. The centers of the Rh$_4$ tetrahedra are located on the origin and center of the unit cell. Only one of the four B$_2$ pairs is indicated. The symbols are as follows: $\bigcirc$, Y; $\circ$, Rh; $\bullet$, B.

rare-earth ions form a tetragonal body-centered lattice with point-group symmetry $\overline{4}2m$ (D_{2d}).[40] The space group is $P4_2/nmc$ (D_{4h}^{15}).

The lattice parameters and c/a ratios are given in Table I. Figure 1 exhibits the proposed structure for YRh$_4$B$_4$. The number of formula units per unit cell is two. The following positions are found: eight Rh atoms in $8g$ —0, x, z, etc., with $x = \frac{1}{4}$ and $z = \frac{1}{8}$; and two Y atoms in $2b$—0,0,$\frac{1}{2}$ and; $\frac{1}{2},\frac{1}{2},0$. The most likely positions for the B atoms are in the eightfold positions $(8g)$ with $x_B = 0.325$, $z_B = 0.847$, etc. The B atoms form pairs parallel to the a axis and are surrounded by five Rh atoms. The Rh lattice consists of tetrahedra with two intermetallic distances of 2.63 Å along the a axis and four slightly larger intermetallic distances, 2.75 Å, caused by an elongation of the tetrahedra along the c axis (Fig. 1). These tetrahedra are connected into sheets perpendicular
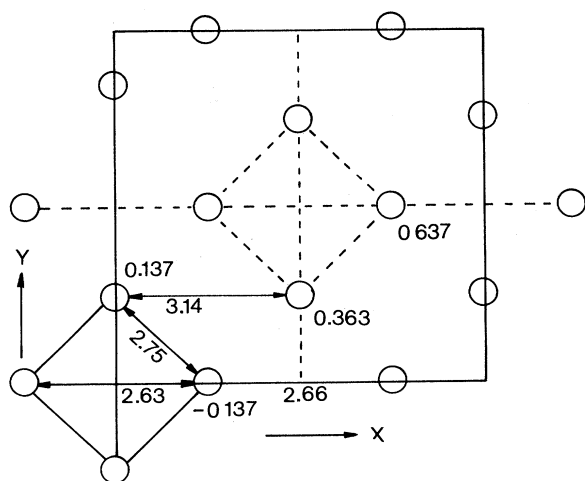
to the c axis through a short intermetallic distance, 2.68 Å, parallel to the a axis. The sheets are held together by the Y atoms through fairly short Y-Rh distances, 2.99 Å (Fig. 2). However, the intermetallic Rh-Rh distance from one sheet to the other is fairly long, namely 3.14 Å.

IV. BRIEF OUTLINE OF THE LUTTINGER-TISZA METHOD USING PERMUTATION GROUPS

Full details of the LT method using permutation groups for the calculation of energies corresponding to the various ferromagnetic and antiferromagnetic arrangements as they apply to this study are described in Ref. 29. Here, a brief outline of the method as it applies to the case of two ions per unit cell, as is the situation with TRRB compounds, is briefly described.

The entire lattice is first divided into 16 sublattices by the application of $\vec{T}^2$ translations ($=2l\vec{a}+2m\vec{b}+2n\vec{c}$; $\vec{a}$, $\vec{b}$, and $\vec{c}$ being the unit-cell vectors, and $a = b$) to the 16 vertices (numbered 1,2,...,16) of two parallelepipeds, each of dimension a, b, and c, with one vertex of each parallelepiped situated at one of the sites of the two RE ions per unit cell, as exhibited in Fig. 3. (For TRRB, $\vec{a}$ and $\vec{b}$ are perpendicular to each other.)

The low-temperature ordered state (in terms of energy) is such that all magnetic moments located on any one of the 16 sublattices are parallel to each other. The relative directions of the magnetic moments of various sublattices are such that the total RE lattice is either ferromagnetic, antiferromagnetic, or layered antiferromagnetic.

Thus the eigenvectors corresponding to these configurations can be expressed as $q(k)\phi_k(\alpha)$, $k=1,2,...,16$; $\alpha=x,y,z$. For the present case the $q(k)$ are 16-dimensional eigenvectors whose (unnormalized) elements are either $+1$ or -1 (parallel or antiparallel), determining

FIG. 2. Projection of the Rh tetrahedra along [001]. The heights of the Rh atoms and intermetallic distances (Å) are indicated. The Rh-Rh distance of 3.14 Å is parallel to the a-c plane only for the ideal value of $x_{Rh} = 0.250$. $\bigcirc$, Rh.

FIG. 3. Two partially overlapping parallelepipeds. Application of $\vec{T}^2$ translations to the 16 vertices as indicated generates the 16 sublattices into which the RE lattice of RRh$_4$B$_4$ is subdivided for the application of the Luttinger-Tisza method.

TABLE II. Unnormalized eigenvectors $q(k)$ of group of permutations P_t $(t=1,2,\ldots,16)$.

the nature of ordering (ferromagnetic or antiferromagnetic). These are listed in Table II. The particular direction in the physical space along which the spins of the kth sublattice point are given by $\phi_k(\alpha)$. The $\phi_k(\alpha)$ are the eigenvectors of a 3×3 matrix L_k, whose components are given as $(\mu,\nu=x,y,z)$

$$L_k^{\mu\nu}=\sum_{j=1}^{16} A_{ij}^{\mu\nu}\epsilon_{P(i,j)}(k) \quad (i=1,2,\ldots,16), \tag{4.1}$$

where $\epsilon_{P(i,j)}(k)$ are the eigenvalues of $q(k)$ under a permutation group of 16 objects, $P(i,j)$ being the permutation containing the cycle (i,j) (listed in Ref. 29). The summation in Eq. (4.1) is independent of i.[29] The matrix elements $A_{ij}^{\mu\nu}$ represent the dipole-dipole and exchange interactions between an ion situated on sublattice i, and all ions on sublattice j, as follows:

$$A_{ij}^{\mu\nu}=\begin{cases}\displaystyle\sum_{l\in\{j\}} J_{il}^{\mu\nu} & \text{for } i\neq j, \\[2ex] \displaystyle\sum_{l\in\{j\},l\neq i} J_{il}^{\mu\nu} & \text{for } i=j,\end{cases} \tag{4.2}$$

where $\{j\}$ represents all ions on sublattice j, and

$$J_{ij}^{\mu\nu}=\frac{S^2}{2}\mu_B^2[g^{\mu\mu}g^{\nu\nu}(r_{ij}^2\delta_{\mu\nu}-3r_{ij}^\mu r_{ij}^\nu)/r_{ij}^5+v_{ij}\Delta_{ij}\delta_{\mu\nu}]. \tag{4.3}$$

In Eq. (4.3), the factor $\frac{1}{2}$ ensures that the energy is not counted twice, S is the ionic spin, μ_B is the Bohr magneton, $g^{\mu\mu}$ is the μth diagonal element of the g tensor (for the present case, the system of coordinate axes is chosen such that it is diagonal), $\vec{r}_{ij}$ is the vector joining the ionic position i to j, r_{ij}^μ is its μth component, $\delta_{\mu\nu}$ is the Kronecker δ function, v_{ij} is the exchange-interaction constant between ions i and j, and $\Delta_{ij}=1$ if i and j are nearest or next-nearest neighbors, and 0 otherwise. Thus, in Eq. (4.3) the first term represents the dipole-dipole interaction, while the second term represents the exchange interaction (considering only the nearest and next-nearest neighbors). One then needs the lattice sums corresponding to the first term of Eq. (4.3). For the present case the required sums are listed in Table III.

The eigenvalues, of course, are those of the 3×3 matrices whose elements are $L_k^{\mu\nu}$ [see Eq. (4.1)] for the various arrangements $q(k)$, $k=1,2,\ldots,16$. The one that corresponds to the lowest energy represents the low-temperature ordering. For the three ferromagnetic orderings $q_1\phi_1(\alpha)$, $\alpha=x,y,z$, one should also take into account the demagnetization contribution if the lattice sums are evaluated over a sphere.[29] This contribution for the present case of a diagonal g tensor is

$$-(4\pi/3)(S^2/2)n_0 g^{\alpha\alpha^2}\mu_B^2, \quad \alpha=x,y,z. \tag{4.4}$$

In Eq. (4.4), n_0 is the number of ions per unit volume, i.e., $2/(a^2c)$ for the present calculation.

V. CRYSTAL FIELD AND THE g FACTORS

Mössbauer spectra have been obtained for compounds with $R=_{66}$Dy, $_{68}$Er, and $_{69}$Tm.[43-45] Well-resolved magnetic-hyperfine-structure spectra are observed in all

TABLE III. Lattice sums over a sphere of radius 500 Å for the lattice of Er ions in ErRh_4B_4. The variables r, x, y, and z are the displacements and their components, from an origin situated at a given ion in sublattice 1 of Fig. 3 to each ion in one of the various $\vec{T}^2$ sublattices. The unit of length is 1 Å. All of the required lattice sums can be obtained from the following five sums. (The z axis is parallel to the c axis, and the x axis is coincident with the $\vec{a}$ vector of the unit cell.)

Sublattice summed	$\sum(3z^2-r^2)/r^5$	$\sum(x^2-y^2)/r^5$	$\sum(xy/r^5)$	$\sum yz/r^5$	$\sum zx/r^5$
1	−0.002 505	0.0	0.0	0.0	0.0
2	−0.014 633	0.012 534	0.0	0.0	0.0
3	−0.014 633	−0.012 534	0.0	0.0	0.0
4	−0.008 901	0.0	0.0	0.0	0.0
5	0.009 346	0.0	0.0	0.0	0.0
6	0.004 385	0.001 102	0.0	0.0	0.0
7	0.004 385	−0.001 102	0.0	0.0	0.0
8	0.002 518	0.0	0.0	0.0	0.0
9	0.002 518	0.0	0.001 35	0.002 084	0.002 084
10	0.002 518	0.0	−0.001 35	0.002 084	−0.002 084
11	0.002 518	0.0	−0.001 35	−0.002 084	0.002 084
12	0.002 518	0.0	0.001 35	−0.002 084	−0.002 084
13	0.002 518	0.0	0.001 35	−0.002 084	0.002 084
14	0.002 518	0.0	−0.001 35	−0.002 084	−0.002 084
15	0.002 518	0.0	−0.001 35	0.002 084	−0.002 084
16	0.002 518	0.0	0.001 35	0.002 084	0.002 084

cases, even above the magnetic transition temperature. The spectra of Dy and Er below their respective magnetic transition temperatures show little change except for a sharpening of some of the lines.[43] This means that the magnetic moments are unchanged and that the magnetic interaction is relatively weak compared to the crystalline-electric-field (CEF) interactions. In all cases,[44,45] the measured moment is near the free-ion value. This shows the presence of a state predominately determined by the angular momentum component $|J_z|=J$ due to the CEF interaction.

The CEF Hamiltonian relevant to the $\bar{4}2m$ symmetry of the RE atom is[22]

$$H_{\text{CEF}}=B_2^0 O_2^0 + B_4^0 O_4^0 + B_6^0 O_6^0 + B_6^4 O_6^4 . \qquad (5.1)$$

In Eq. (5.1) the O_l^m are spin operators as defined by Abragam and Bleaney.[46] If the exchange interaction is assumed to be isotropic, then the CEF determines the anisotropy.

The g values for the various RE ions in TRRB compounds have not been experimentally determined. However, they may be estimated from the Hund's-rule ground state provided that the B_l^m for the various RE ions as given by Eq. (5.1) are known. These can be estimated as follows.[47]

The B_l^m have been determined experimentally for $R=$ Er from Schottky specific-heat data[47] and Mössbauer data.[22-24] Now, the relationship between B_l^m and A_l^m, the crystal-field parameters, which are the same for all RE's, is noted, i.e.,

$$B_l^m=\alpha_l\langle r^l\rangle A_l^m . \qquad (5.2)$$

In Eq. (5.2), α_l is the Stevens's factor[26] whose value is known, but dependent on the particular rare-earth ion

under consideration, and $\langle r^l\rangle$ is a $4f$ integral obtained from Hartree-Fock atomic calculation. In this form, the A_l^m are determined by charge distribution over the lattice and are presumed to be approximately independent of the particular rare-earth ion in an isostructural series of compounds.[26] The factors α_l and the expectation values $\langle r^l\rangle$ are listed by Abragam and Bleaney.[46] In this way the B_l^m for all RE ions can be estimated. With the appropriate B_l^m for a given RE ion, one can diagonalize the $(2J+1)^2$ matrix for the H_{CEF} as given by Eq. (5.1). ($\vec{J}=\vec{L}+\vec{S}$, J, L, and S being the total, orbital, and spin angular momenta, respectively.) For the eigenvectors of the lowest-lying doublet, one then diagonalizes the 2×2 matrices for J_z and J_x and finds the differences of the resulting eigenvalues denotes as $\epsilon_{||}$ and $\epsilon_{\perp}$, respectively. The g factors are then[46]

$$g_{||}=2\Lambda\epsilon_{||}$$

and   (5.3)

$$g_{\perp}=2\Lambda\epsilon_{\perp} ,$$

and the values of Λ for different RE ions are listed by Abragam and Bleaney.[46]

The resulting $g_{||}$ and $g_{\perp}$ values as calculated by Staveren et al.[48] are listed in Table IV. (It should be noted that for Tm^{3+} the lowest CEF state is nondegenerate, and then the g factors in Table IV are those calculated for the doublet that lies just above this state.)

VI. CALCULATED LOW-TEMPERATURE ORDERINGS

For the application of the LT method one requires the lattice sums of Eq. (4.3), as given in Table III for $R=$ Er

TABLE IV. Values of $g_{\parallel}$ and $g_{\perp}$ (as calculated), predicted orderings on the basis of the dipole-dipole interaction, and experimentally observed orderings for the various $R\text{Rh}_4\text{B}_4$ compounds. An asterisk on the predicted ordering indicates that with appropriate values of exchange-interaction constants the predicted ordering will be in agreement with that observed experimentally (see Sec. VI). FM denotes ferromagnetic, AF denotes antiferromagnetic, and super denotes superconducting.

Re	Hund's-rule ground state $(^{2S+1}L_J)$	$g_{\parallel}$	$g_{\perp}$	Predicted ordering	Observed ordering
$_{58}\text{Ce}^{3+}(4f^1)$	$^2F_{5/2}$	4.28	0.126	c-axis FM	
$_{59}\text{Pr}^{3+}(4f^2)$	$^3H_4$	4.80	0	c-axis FM	
$_{60}\text{Nd}^{3+}(4f^3)$	$^4I_{9/2}$	6.51	0.073	c-axis FM*	AF super (c axis)
$_{61}\text{Pm}^{3+}(4f^4)$	$^5I_4$	0	0		
$_{62}\text{Sm}^{3+}(4f^5)$	$^6H_{5/2}$	0.286	0.857	basal-plane FM*	AF super (c axis)
$_{63}\text{Eu}^{3+}(4f^6)$	$^7F_0$	0	0		
$_{64}\text{Gd}^{3+}(4f^7)$	$^8S_{7/2}$	14	0	c-axis FM	FM (c axis)
$_{65}\text{Tb}^{3+}(4f^8)$	$^7F_6$	18.0	0	c-axis FM	FM (easy axis c)
$_{66}\text{Dy}^{3+}(4f^9)$	$^6H_{5/2}$	20.0	0	c-axis FM	FM (easy axis c)
$_{67}\text{Ho}^{3+}(4f^{10})$	$^5I_8$	20.0	0	c-axis FM	FM (easy axis c)
$_{68}\text{Er}^{3+}(4f^{11})$	$^4I_{15/2}$	0.937	9.219	basal-plane FM	FM (easy axis a)
$_{69}\text{Tm}^{3+}(4f^{12})$	$^3H_6$	1.318[a]	0[a]	c-axis FM*	AF (easy axis a)
$_{70}\text{Yb}^{3+}(4f^{13})$	$^2F_{7/2}$	1.142	4.571	basal-plane FM	

[a]The doublet that lies just above the lowest-lying singlet has been used for the calculation of g values.

(the same lattice sums are used for other RE compounds due to the close proximity of unit-cell parameters). Furthermore, the g values (listed in Table IV) are also required. The coordinate system chosen is such that the z axis is parallel to the c axis, and the x axis is coincident with the vector $\vec{a}$ of the unit cell. The values of the exchange constants between the various RE ions are not known. However, an upper limit can be set for their values if the predicted orderings are to be in agreement with the observed low-temperature orderings.

Without explicitly taking into account the numerical values of the g factors and the exchange constants, the energies per ion for the two lowest-lying states can be calculated using the LT method, as described in Sec. V, to be as follows. (Of course, their relative values can be determined only when the numerical values for the g factors and the exchange constants are explicitly taken into account.) Specifically, then, these energies are, per ion, in K,

$$q(1): \quad E_{Azz} = -0.003\,18g_{\parallel}^2 + 2v_{NN} + v_{NNN}, \quad (6.1)$$

$$q(13) \text{ or } q(14): \quad E_{Bzz} = -0.001\,63g_{\parallel}^2 - v_{NNN}, \quad (6.2)$$

$$q(1): \quad E_{Axx} = E_{Ayy} = -0.003\,17g_{\perp}^2 + 2v_{NN} + v_{NNN}, \quad (6.3)$$

$$q(11) \text{ or } q(12): \quad E_{Bxx} = E_{Byy} = -0.002\,69g_{\perp}^2. \quad (6.4)$$

In Eqs. (6.1)—(6.4), $g_{\parallel}$ and $g_{\perp}$ denote the g factors along the z and x (or y) axes, respectively. (The g tensor is diagonal for the present case: $g_{\parallel} = g_{zz}$, and $g_{\perp} = g_{xx} = g_{yy}$.) v_{NN} and v_{NNN} (in K) are the nearest-neighbor (NN) (distance $1-4 = 5.231$ Å for Tm; Fig. 3) and next-nearest-neighbor (NN) (distance $= 1-2 = 1-3 = \cdots = 5.287$ Å for Tm) exchange-interaction constants, respectively; and the subscripts A and B refer to the two lowest-lying states (in energy), while the subscripts xx, yy, and zz denote the physical directions in which the spins point. [The demagnetization corrections for ferromagnet-

ic orderings have already been incorporated in Eqs. (6.1) and (6.3).]

From (6.1)—(6.4) it is clear that when the spins point in the z direction the ferromagnetically (FM) ordered state E_{Azz} lies lower in energy than the layered antiferromagnetic (LAF) [$q(13)$ or $q(14)$ for spins pointing along x, or $q(15)$ or $q(16)$ for spins pointing along y] state, as long as the NN and NNN exchange-interaction constants are such that, in units of K,

$$v_{NN} + v_{NNN} < 0.000\,77g_{\parallel}^2. \quad (6.5)$$

When the spins point in the x (or y) direction, the FM state lies lower in energy than the LAF states $q(11)$ or $q(12)$ as long as

$$2v_{NN} + v_{NNN} < 0.000\,48g_{\perp}^2, \quad (6.6)$$

in units of K. It is, of course, to be noted from (6.5) and (6.6), that the spins in the lowest-energy state point in the z or x (or y) direction depending upon the $g_{\parallel}$ value relative to $g_{\perp}$ value.

Finally, if the exchange interaction was completely absent, then on the basis of the dipole-dipole interaction alone, the FM ordering along the z direction would have a lower energy than that along the x (or y) direction provided that

$$g_{\parallel} > 0.998g_{\perp}. \quad (6.7)$$

Cognizant of Eqs. (6.5)—(6.7), one can now predict the ordering that will be favored energetically at low temperatures on the basis of dipole-dipole interactions alone using the g factors as estimated in Sec. IV and listed in Table IV. These orderings are also listed in Table IV. They are all found to be ferromagnetic with spin orientations either along the z (or c) axis, or in the plane perpendicular to the c (basal-plane) axis. It should be noted that the energy corresponding to spin orientations anywhere in the $x - y$

(basal) plane is the same. It is found that, for $R = {}_{65}$Tb, ${}_{66}$Dy, ${}_{67}$Ho, and ${}_{68}$Er, these orderings agree with those observed experimentally. (Table IV also contains the observed orderings.) For the cases $R = {}_{60}$Nd, ${}_{62}$Sm, and ${}_{69}$Tm, the predicted orderings could all be antiferromagnetic to agree with those observed experimentally, provided that the values of v_{NN} and v_{NNN} are such that the inequalities (6.5) and (6.6) above are *not* satisfied. In particular, the following should be noted.

(i) Tm^{3+}: If $v_{NN} + v_{NNN} > 1.3435 \times 10^{-3}$ K, then the LAF states $q(13)$ and $q(14)$ lie lowest in energy.

(ii) Nd^{3+}: If $2v_{NN} + v_{NNN} > 32.6 \times 10^{-3}$ K, then the LAF states $q(13)$ and $q(14)$ lie lowest in energy.

(iii) Sm^{3+}: If $2v_{NN} + v_{NNN} > 0.3525 \times 10^{-3}$ K, then the LAF states $q(11)$, $q(12)$, $q(15)$, and $q(16)$ lie lowest in energy.

VII. MAGNETIC FIELD AT RHODIUM SITE

It is plausible that if the magnetic field due to RE ions at rhodium sites (whose $3d$ electrons are responsible for superconductivity) is less than the superconductivity-quenching value, then the superconductivity can coexist with the magnetic ordering. It is the object of this section to estimate this field.

With the use of the standard expression for the magnetic field due to a dipole at a distance $\vec{r}$, the magnetic field components $h_{\alpha\beta}$ ($\beta = x, y, z$) due to the dipole pointing in the direction α ($= x, y, z$) can be expressed as

$$h_{\alpha\beta} = \mu_B S g^{\alpha\alpha} (3r_\alpha r_\beta - \delta_{\alpha\beta} r^2)/r^5 . \tag{7.1}$$

In (7.1), r_α and r_β are the α and β components of $\vec{r}$, while r is its magnitude.

Using (7.1) for the various orderings, where all the dipoles on a sublattice point either parallel or antiparallel to the direction α as dictated by the elements of the eigenvectors $q(k)$, denoted as $q(k,j)$, $j = 1, 2, \ldots, 16$, describing the particular ordering ($+1$ or -1; see Table II), the following expressions can be obtained for the β component of the total magnetic field $\vec{h}_\alpha^k$, due to the ordering described by $q(k)$ at a Rh site, chosen to be at the origin:

$$h_{\alpha\beta}^k = \begin{cases} \mu_B S g^{\alpha\alpha} \sum_{j=1}^{16} \left[\sum_i 3r_{i\alpha}^k r_{i\beta}^k / r_i^{k^5} \right] q(k,j) \\ \quad \text{for } \beta \neq \alpha \\ \\ \mu_B S g^{\alpha\alpha} \sum_{j=1}^{16} \left[\sum_i (3r_{i\alpha}^{k^2} - r_i^{k^2}) / r_i^{k^5} \right] q(k,j) \\ \quad \text{for } \beta = \alpha . \end{cases}$$

$$\text{(7.2)} \qquad \text{(7.3)}$$

In Eqs. (7.2) and (7.3) the subscript i covers all of the dipoles of a sublattice k, and r_i^k is the distance of ion i on sublattice k from the origin (and subscript α and β denote its α and β components, respectively). In writing (7.2) and (7.3), the fact that for the origin on a rhodium site the RE ions on various sublattices are located such that for every $\vec{r}_i^k$ (origin to RE ion), there is another i (say, j) such that $\vec{r}_j^k = -\vec{r}_i^k$, has been taken into account.

For use in Eqs. (7.2) and (7.3), lattice sums are required; those for ErRh$_4$B$_4$ are given in Table V. (The same lattice sums can be used for all RE's due to the close proximity of unit-cell parameters.) It should be noted that for ferromagnetic ordering the lattice sums should be performed over a thin long cylinder along the direction of magnetization since the ferromagnetic ordering takes place in the form of thin long needles (to minimize energy).[49] This amounts to adding $-4\pi\rho/3$ to the lattice sums of the type $\sum_i (3r_{i\alpha}^2 - r_i^2)/r_i^5$, where $\rho = (8a^2c)^{-1}$ is the density of ions on a $\vec{T}^2$ sublattice (dimensions of the unit cell are $2a$, $2a$, and $2c$).

The lowest-energy configuration of RE ions, as determined in Sec. VI, is found to be any one of the configurations $q(1)$, $q(11)$, $q(12)$, $q(13)$, $q(14)$, $q(15)$, or $q(16)$ depending upon the g factors and the exchange constants. Table VI lists the values of the magnetic fields (in units of

TABLE V. Lattice sums from rare-earth–ion positions over a sphere of radius 500 Å at a Rh site as the origin for ErRh$_4$B$_4$. For further details (units, etc.), see the caption of Table III.

Sublattice summed	$\sum (3z^2 - r^2)/r^5$	$\sum (x^2 - y^2)/r^5$	$\sum xy/r^5$	$\sum yz/r^5$	$\sum zx/r^5$
1	−0.007 193	0.160 800	0.0	0.0	0.111 800
2	−0.016 755	0.016 348	0.0	0.0	−0.002 812
3	−0.012 025	−0.009 188	0.0	0.0	0.000 400
4	−0.008 807	−0.001 130	0.0	0.0	−0.000 291
5	0.009 196	0.000 222	0.0	0.0	−0.000 379
6	0.004 950	0.001 112	0.0	0.0	0.000 307
7	0.003 899	−0.001 067	0.0	0.0	−0.000 127
8	0.002 521	−0.000 174	0.0	0.0	0.000 118
9	0.004 360	−0.005 281	0.002 949	0.006 298	0.003 238
10	−0.003 605	0.002 284	−0.001 303	0.001 315	−0.001 509
11	0.004 360	−0.005 281	−0.002 949	−0.006 298	0.003 238
12	−0.003 605	0.002 284	0.001 303	−0.001 315	−0.001 509
13	0.007 200	−0.001 321	0.000 551	−0.001 995	−0.001 067
14	0.001 826	0.000 953	−0.000 384	−0.000 739	0.000 771
15	0.007 200	−0.001 321	−0.000 551	0.001 995	−0.001 067
16	0.001 826	0.000 953	0.000 384	0.000 739	0.000 771

TABLE VI. Magnetic field components at an Rh site due to the seven possible lowest-lying (in energy) ferromagnetic and antiferromagnetic orderings $q(k)$ of the rare-earth ions $R\text{Rh}_4\text{B}_4$. The same lattice sums have been assumed for all RE's due to the close proximity of unit-cell parameters. $h_{\alpha\beta}$ means the β component of the magnetic field when all the spins point parallel and antiparallel to the α direction $(\alpha,\beta=x,y,z)$ depending on the particular ordering. The units are such that actual values in gauss are obtained by multiplying each $h_{\alpha\beta}$ by $g^{\alpha\alpha}$ (listed in Table IV).

Ordering	h_{xx}	h_{xy}	h_{xz}	h_{yx}	h_{yy}	h_{yz}	h_{zx}	h_{zy}	h_{zz}
$q(1)$	936	0	1556	0	-1292	0	1556	0	-210
$q(11)$	1037	92	1590	92	-1083	174	1590	174	46
$q(12)$	1082	26	1477	26	1025	-35	1477	-35	-58
$q(13)$	1024	144	1578	144	-1097	104	1578	104	73
$q(14)$	1069	-26	1465	-26	-1038	35	1465	35	-31
$q(15)$	873	0	1799	0	-901	0	1799	0	27
$q(16)$	1000	-118	1546	-118	-1083	-139	1546	-139	83

$g_{\parallel}$ gauss and $g_{\perp}$ gauss; see caption) due to these configurations at a rhodium site. For a specific RE, one need only multiply by the appropriate g factors, given in Table IV.

As a particular example, one can estimate the magnetic field at a rhodium site for $R=_{69}\text{Tm}$. Here, the observed low-temperature ordering is LAF, namely that described by either $q(13)$ or $q(14)$ with equal probability (see Sec. VI) of the spins pointing either parallel or antiparallel to the z direction ($g_{\parallel}=1.38$, $g_{\perp}=0$). For the $q(13)$ configuration, the magnetic field components at a rhodium site are found to be $h_{zx}=2080$ G, $h_{zy}=137$G, and $h_{zz}=96$ G, while for the $q(14)$ configuration these are $h_{zx}=1931G$, $h_{zy}=46$ G, and $h_{zz}=41$ G. Values of anywhere from 1 to 6 kG, or even as large as 12 kG, are found for superconductivity-quenching fields.[13,14,50] Thus, the above-mentioned values for $h_{\alpha\beta}$ in $R=_{69}\text{Tm}$ at a rhodium site appear to have the magnitude that would permit coexistence of superconductivity and magnetic ordering in $R=_{69}\text{Tm}$. Similar considerations can be applied to the other TRRB compounds.

VIII. CONCLUDING REMARKS

The calculations of the present paper indicate that with appropriate values of nearest-neighbor and next-nearest-neighbor exchange constants (in addition to, of course, the dipole-dipole interaction), the observed antiferromagnetic orderings for $R=_{60}\text{Nd}$, $_{68}\text{Sm}$, and $_{69}\text{Tm}$ can all be ac-

counted for. As for the observed ferromagnetic orderings, these can all be accounted for solely by dipole-dipole interaction between the RE ions.

It is to be noted that this paper does not account for the *finer* details of magnetic orderings as discussed in Sec. II. These are, namely, the oscillatory character of magnetization, spiral magnetization state in a ferromagnetic superconductor, vortex structure, combined spiral magnetic and spontaneous vortex states, and laminar structure. They should be accounted for by additional mechanisms, e.g., q-dependent magnetic susceptibility,[34] electromagnetic interaction between the magnetization of the localized ions and the momenta of conduction electrons,[35] and the RKKY indirect-exchange mechanism.[17] It is hoped that the present results will be helpful in further developing the understanding of the phenomena of superconductivity and magnetic ordering as they occur in $R\text{Rh}_4\text{B}_4$.

[1]*Superconductivity in Ternary Compounds II,* edited by M. B. Maple and Ø. Fischer (Springer, Berlin, 1982).

[2]M. Ishikawa and Ø. Fischer, Solid State Commun. **24,** 747 (1977).

[3]D. E. Moncton, G. Shirane, W. Thomlinson, M. Ishikawa, and Ø. Fischer, Phys. Rev. Lett. **41,** 1133 (1978).

[4]C. F. Majkrzak, G. Shirane, W. Thomlinson, M. Ishikawa, Ø. Fischer, and D. E. Moncton, Solid State Commun. **31,** 773 (1979).

[5]W. Thomlinson, G. Shirane, D. E. Moncton, M. Ishikawa, and Ø. Fischer, Phys. Rev. B **23,** 4455 (1981).

[6]R. W. McCallum, D. C. Johnston, R. N. Shelton, and M. B. Maple, Solid State Commun. **24,** 391 (1977).

[7]M. B. Maple, L. D. Woolf, C. F. Majkrzak, G. Shirane, W. Thomlinson, and D. E. Moncton, Phys. Lett. **77A,** 487 (1980).

[8]H. C. Hamaker, L. D. Woolf, H. B. MacKay, Z. Fisk, and M. B. Maple, Solid State Commun. 31, 139 (1979).

[9]H. C. Hamaker, L. D. Woolf, H. B. MacKay, Z. Fisk, and M. B. Maple, Solid State Commun. 32, 289 (1979).

[10]Ø. Fischer, M. Ishikawa, M. Pelizzone, and A. Treyvaud, J. Phys. (Paris) Colloq. **40,** C5-89 (1979).

[11]M. B. Maple, J. Phys. (Paris) Colloq. **39,** C6-1374 (1978).

[12]M. Ishikawa, Ø. Fischer, and J. Muller, J. Phys. (Paris) Colloq. **39,** C6-1379 (1978).

[13]H. C. Hamaker, H. B. MacKay, L. D. Woolf, M. B. Maple,

W. Odoni, and H. R. Ott, Phys. Lett. A81, 91 (1981).

[14]H. C. Hamaker, H. B. MacKay, M. S. Torikachvili, L. D. Woolf, and M. B. Maple, J. Low Temp. Phys. 44, 553 (1981).

[15]C. F. Majkrzak, D. E. Cox, G. Shirane, H. A. Mook, H. C. Hamaker, H. B. MacKay, Z. Fisk, and M. B. Maple, Phys. Rev. B 26, 245 (1982).

[16]H. Matsumoto and H. Umezawa, Cryogenics 37 (1983).

[17]C. F. Majkrzak, S. K. Satija, G. Shirane, H. C. Hamaker, Z. Fisk, and M. B. Maple, Phys. Rev. B 27, 2889 (1983).

[18]F. Acker and H. C. Ku, J. Low Temp. Phys. 42, 449 (1981).

[19]H. B. MacKay, L. D. Woolf, M. B. Maple, and D. C. Johnston, J. Low Temp. Phys. 41, 639 (1980).

[20]W. Odoni, H. R. Ott, and M. B. Maple, J. Low Temp. Phys. 51, 505 (1983).

[21]M. Ishikawa, Contemp. Phys. 23, 443 (1982).

[22]B. D. Dunlap and D. Niarchos, Solid State Commun. 44, 1577 (1982).

[23]H. B. Radonsky, B. D. Dunlap, G. S. Knapp, and D. G. Niarchos, Phys. Rev. B 27, 5526 (1983).

[24]G. K. Shenoy, D. R. Noakes, and D. G. Hinks, Solid State Commun. 42, 411 (1982).

[25]G. W. Crabtree, F. Behroozi, S. A. Campbell, and D. G. Hinks, Phys. Rev. Lett. 49, 1342 (1982).

[26]Handbook on the Physics and Chemistry of Rare Earths, edited by K. A. Gschneider, Jr. and L. Eyring (North-Holland, Amsterdam, 1979), Vol. 2.

[27]S. Hüfner, Optical Spectra of Transparent Rare Earth Compounds (Academic, New York, 1978), pp. 40—55.

[28]J. M. Luttinger and L. Tisza, Phys. Rev. 70, 954 (1946).

[29]S. K. Misra, Phys. Rev. B 8, 2026 (1973); J. Felsteiner and S. K. Misra, ibid. 8, 253 (1973).

[30]D. E. Moncton, G. Shirane, and W. Thomlinson, J. Magn. Magn. Mater. 14, 172 (1979), and references cited therein.

[31]H. R. Ott, W. Odoni, H. C. Hamaker, and M. B. Maple, Phys. Lett. 75A, 243 (1980).

[32]W. A. Fertig, D. C. Johnston, L. E. DeLong, R. W. McCallum, M. B. Maple, and B. T. Matthias, Phys. Rev. Lett. 38, 987 (1977); D. E. Moncton, D. B. McWhan, J. Eckert, G.

Shirane, and W. Thomlinson, ibid. 39, 1164 (1977).

[33]L. D. Woolf, M. Tovar, H. C. Hamsker, and M. B. Maple, Phys. Lett. 72A, 481 (1979).

[34]P. W. Anderson and H. Suhl, Phys. Rev. 116, 898 (1959).

[35]E. I. Blount and C. M. Varma, Phys. Rev. Lett. 42, 1079 (1979).

[36]S. K. Sinha, G. W. Crabtree, D. G. Hincks, and H. A. Mook, Phys. Rev. Lett. 48, 950 (1982).

[37]H. S. Greenside, E. I. Blount, and C. M. Varma, Phys. Rev. Lett. 46, 49 (1981).

[38]M. Tachiki, in Proceedings of the 16th International Conference on Low Temperature Physics [Physica 109 & 110B, 1699 (1982)].

[39]C. R. Hu and T. E. Ham, Physica 108B, 1041 (1981).

[40]J. M. Vandenberg and B. T. Matthias, Proc. Natl. Acad. Sci. U.S.A. 74, 1336 (1977).

[41]Yu B. Kuz'ma and N. S. Bilonizhko, Kristallografiya 16, 1031 (1971) [Sov. Phys.—Crystallogr. 16, 897 (1972)].

[42]J. M. Vandenberg, B. T. Matthias, E. Corenzwit, and H. Barz, Mater. Res. Bull. 10, 889 (1975).

[43]G. K. Shenoy, B. D. Dunlap, F. Y. Fradin, S. K. Sinha, C. W. Kimball, W. Potzel, F. Pröbst, and G. M. Kalvius, Phys. Rev. 21, 3886 (1980).

[44]G. K. Shenoy, B. D. Dunlap, F. Y. Fradin, and C. W. Kimball, Bull. Am. Phys. Soc. 23, 206 (1978).

[45]G. K. Shenoy, P. J. Viccaro, D. Niarchos, J. D. Cashion, B. D. Dunlap, and F. Y. Fradin, in Ternary Superconductors, edited by G. K. Shenoy, B. D. Dunlap, and F. Y. Fradin (North-Holland, Amsterdam, 1981), p. 163.

[46]A. Abragam and B. Bleaney, Electron Paramagnetic Resonance of Transition Metal Ions (Clarendon, Oxford, 1970).

[47]L. D. Woolf, D. C. Johnston, H. B. MacKay, R. W. McCallum, and M. B. Maple, J. Low Temp. Phys. 35, 651 (1979).

[48]M. V. Staveren and H. Andriessen (private communication).

[49]C. Kittel, Phys. Rev. 82, 965 (1951).

[50]H. R. Ott, W. A. Fertig, D. C. Johnston, and M. B. Maple, J. Low Temp. Phys. 33, 159 (1958).